Journal of Optoelectronics and Advanced Materials Vol. 5, No. 2, June 2003, p. 503 - 510

CORROSION RESISTANCE OF TiN COATED 316L STAINLESS STEEL IN ARTIFICIAL PHYSIOLOGICAL SOLUTION

M. Braic, S. Zamfir[a], M. Balaceanu[*], V. Braic, G. Pavelescu, A. Zamfir[a], A. Vladescu

National Institute for Optoelectronics, Bucharest, Romania
[a]"Politehnica" University of Bucharest, Romania

The corrosion behavior of TiN coated 316L stainless steel in an artificial physiological solution was investigated by means of an electrochemical test. Two different PVD methods were used for film deposition: cathodic arc and reactive magnetron sputtering. The dependence of the corrosion resistance on the main deposition parameters (nitrogen pressure, substrate bias) was analyzed. For a better characterization of the investigated coatings, other characteristics, like elemental composition, phase composition, texture, microhardness, adhesion to the substrate were determined.

(Received January 21, 2003; accepted after revision May 8, 2003)

Keywords: Corrosion resistance, TiN coatings, PVD methods

1. Introduction

The selection of biocompatible materials is based on their biocompatibility and their biofunctionality. The first characteristic refers to the implant effect on the surrounding tissue and the second one to its capability to assume the function of the replaced biologic system. In practice, both properties are closely interdependent and are connected to wear-corrosion resistance of the materials. If the implant rejection as a result of mechanical imperfections is relatively rare, most failures are caused by a lack of biocompatibility which is directly related to the corrosion resistance of the implant [1], [2].

In order to find the most adequate materials to be used as implants in living tissue, many alloys have been developed, beginning with austenitic stainless steels [3]. In general, the austenitic stainless steels 316 and 316L have good corrosion resistance and the additional alloying with molybdenum decreases their susceptibility to pitting corrosion. Nevertheless, in certain cases (in strongly stressed or nonoxigenated environments) stainless steels are affected by corrosion. Moreover, these types of steel have a low wear resistance. The performance of implants made of stainless steel could be improved if they were coated with thin films of materials offering protection against corrosion and wear. Among these coatings, TiN would be a suitable choice, due to its remarkable properties such as high microhardness, chemical inertness, high wear and abrasion resistance [4]-[6].

The goal of this work was to investigate the corrosion behavior of TiN coated 316L stainless steel in artificial physiological solution. Two techniques were used for TiN deposition (cathodic arc method (c.a.m.) and reactive magnetron sputtering method (r.m.s.m.)), in order to select the most suitable system for preparation of anticorrosive coatings. For each method, the influence of the main deposition parameters (N_2 pressure, substrate bias) on the corrosion resistance of the TiN films was examined. Additional information on the film characteristics was obtained by elastic recoil detection (ERD) and X-ray diffraction (XRD) analyses, microhardness and thickness measurements and adhesion tests.

---

[*] Corresponding author: balaceanu@inoe.inoe.ro

2. Experimental

The experimental devices for c.a.m. and r.m.s.m. have been described in detail elsewhere [7], [8]. The main process parameters for both deposition methods are summarized in Table 1. The N_2 pressure was measured with an ion gauge calibrated with a capacitance manometer and was kept constant during the deposition process, using a mass flow rate controller.

Table 1. Deposition parameters for TiN coatings prepared by c.a.m. and r.m.s.m.

Sample No.	Deposition method	P_{N2} (Pa)	I_a (A)	I_m (A)	V_s (V)	T (°C)	t (min)
1	c.a.m.	1×10^{-2}	90	-	220	340	60
2	c.a.m.	1×10^{-1}	90	-	220	340	60
3	c.a.m.	1×10^{0}	90	-	220	370	60
4	c.a.m.	3×10^{-1}	90	-	0	190	60
5	c.a.m.	3×10^{-1}	90	-	90	280	60
6	c.a.m.	3×10^{-1}	90	-	220	350	60
7	r.m.s.m	1×10^{-1}	-	2.5	50	180	120
8	r.m.s.m	3×10^{-1}	-	2.5	50	180	120
9	r.m.s.m	5×10^{-1}	-	2.5	50	180	120
10	r.m.s.m	3×10^{-1}	-	2.5	20	145	120
11	r.m.s.m	3×10^{-1}	-	2.5	100	205	120

P_{N2} – nitrogen pressure, I_a – arc current, I_m – magnetron current, V_s – substrate bias,
T – substrate temperature, t – deposition time

The chemical composition of the films was investigated by ERD technique, using an incident 80 MeV Cu^{10+} ion beam. The detector of the elastically scattered recoils consisted of a ΔE pulse ionization chamber and a residual energy silicon detector placed inside the ionization chamber. Phase composition and texture were studied by XRD analysis using an X-ray DRON diffractometer with Cu K_α radiation.

Microhardness (Vickers) measurements were performed by means of a microhardness tester at 20 g load. Film thickness was determined by optical microscope examination of the cross section through the coating. Scratch tests under standard conditions were undertaken to evaluate the coating adhesion. Surface topography of the films was examined by optical microscopy.

Corrosion resistance was investigated by an electrochemical test (open circuit potential (OCP) measurements), using a PHOM 4 pH/mV-meter. As an electrolyte, an artificial physiological solution at room temperature was used. The chemical composition of the corrosive environment is given in Table 2. Corrosion behavior was appreciated by measuring time dependent variation of the free corrosion potential Vcorr (test duration – 360 min). The potential was measured with respect to a Calomel reference electrode. The testing cell also contained a thermocouple and an electrode for pH determination. This technique allows evaluating the corrosion behavior of various materials (e.g. [9]). The value of the free corrosion potential at moment zero is a specific parameter for a certain material. In general, a more positive potential indicates a better corrosion resistance and the trend of the potential evolution with time shows the relative importance of the activation and passivation effects specific to a certain corrosion process. Moreover, the corrosion phenomena (pitting, crevice corrosion) taking place during the corrosion attack can be evidenced.

Table 2. Chemical composition of the artificial physiological solution.

Compound	Concentration (g/l)
NaCl	8.44
$NaHCO_3$	0.35
NaH_2PO_4	0.06
$NaH_2PO_4 \cdot H_2O$	0.06

The samples for the corrosion test, consisting of square plates (23 × 23 × 4 mm) made of 316L stainless steel, were carefully polished and ultrasonically cleaned with thrichloroethylene. The coated specimens were masked with wax to expose surfaces of the same area magnitude (~100 mm^2) and similar substrate polishing. Prior to deposition, the samples were sputtered by Ti ion bombardment (1000 V; 5 min).

3. Results and discussion

3.1. Film characteristics

A typical example of ERD spectra from a TiN film prepared by c.a.m. is shown in Fig. 1, where the computer simulation curve is also plotted (deposition condition: $P_{N2} = 10^{-2}$ Pa, $V_s = 220$ V, $I_a = 90$ A). In this case the film composition was: Ti – 44.6%, N – 53.5 %, O – 1.3 %, C – 0.6 %, from which an N/Ti ratio of 1.2 was calculated. The presence of a small amount of oxygen and carbon is due both to residual gas incorporated in the chamber walls and to the film contamination during the sample handling in open atmosphere before the composition analysis.

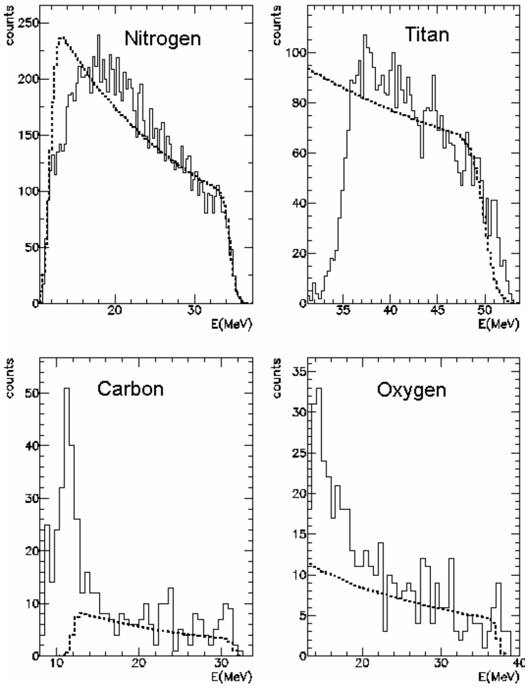

Fig. 1. ERD spectra of Ti,N,O and C for TiN coating prepared by c.a.m.

The dependence of the N/Ti ratio on the nitrogen pressure for the TiN films prepared under the deposition conditions described in Table 1 are given in Table 3. It can be seen that in the case of the c.a.m. coatings the deposition parameters only slightly influenced the film stoichiometry, while for the r.m.s.m. coatings the N/Ti ratio significantly increases with the increase of the N_2 pressure and with the decrease of the substrate bias.

Table 3. N/Ti ratio for the TiN coatings.

Sample no.	1	2	3	4	5	6	7	8	9	10	11
N/Ti	1.2	1.27	1.3	1.32	1.29	1.29	0.82	1.08	1.19	1.2	0.95

Two typical X-ray diffraction patterns for c.a.m. and r.m.s.m. coatings are illustrated in Fig. 2a and b, respectively. Both layers exhibit a strong (111) preferred orientation, as it was commonly reported for the films deposited by these methods [4], [10]. This particular orientation was predicted in the deposition conditions in which the strain energy was dominant as compared to the surface energy [11], [12].

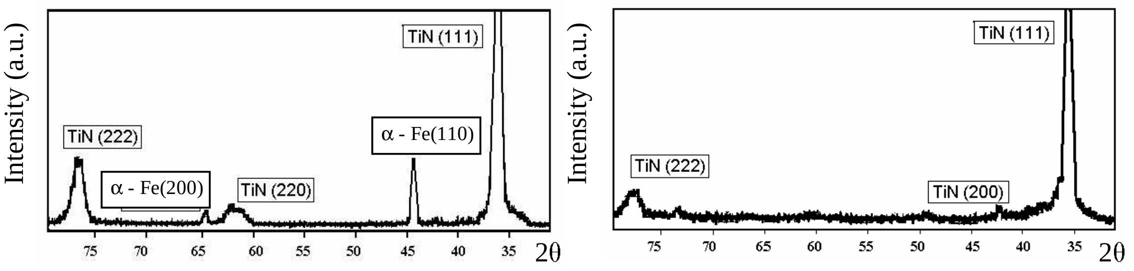

a) c.a.m films

b) r.m.s.m. films

Fig. 2. X-ray diffraction patterns for TiN coatings.

Microhardness measurements showed that higher microhardness values were obtained for the films deposited by c.a.m. Maximum microhardness of 2600-2800 $HV_{0.02}$ and 2000-2200 $HV_{0.02}$ were measured for c.a.m. and r.m.s.m. films, respectively. The measurements of the film thickness revealed that for both deposition methods the deposition rate increased almost linearly with the discharge current and depended only slightly on the nitrogen pressure and on the substrate bias, as already reported [7]. The films prepared for the corrosion tests had thicknesses in the range 1.8 – 2.2 μm.

The scratch tests showed that the adhesion depends on the substrate characteristics (material, surface preparation and cleaning, hardness) and on the film properties (thickness, microhardness). The critical load increased with the film microhardness and thickness and with the substrate hardness. For the films deposited on stainless steel substrates, critical loads of 28 – 34 N were measured. The experiments did not reveal significant differences between the adhesion of the TiN coatings prepared by either c.a.m. or r.m.s.m.

3.2. Corrosion resistance of TiN films

The corrosion behavior of TiN films deposited on 316L stainless steel by c.a.m. and r.m.s.m. is illustrated in Figs. 3, 4 and 6, 7, respectively. One may observe the influence of the main process parameters (P_{N2} and V_s) on the corrosion resistance of the coatings.

For the uncoated sample (Fig. 3), the activation and passivation effects are reciprocally compensated very soon after the beginning of the experiment.

It is important to note that the corrosion resistance of the coatings strongly depended on the deposition conditions for both methods. For interpretation of the corrosion behavior of various coatings, the influence of the deposition parameters on the chemical composition, surface topography and morphology of the films was taken into account.

3.3. Cathodic arc deposited film

As shown in Fig. 3, where the dependence of the corrosion resistance on the N_2 pressure is presented, the best corrosion behavior was found in the case of the film deposited at the highest N_2 pressure (1 Pa), for which a low corrosion activity can be observed. With the increasing duration of the corrosive attack the potential became more cathodic and, as a result of the occurrence of insoluble corrosion products on the film surface, a passive thin film was formed. The passivation occurs at relatively high positive values of the potential, which shows that the coated sample is nobler that the uncoated one. For the films deposited at lower pressures (10^{-1} and 10^{-2} Pa) the corrosion process is active during the entire testing time. The sharp fluctuations of the potential (for the coating prepared at 10^{-1}Pa) indicate a significant localized corrosion (pitting), while for the sample 1 (10^{-2} Pa) the potential variations suggest a crevice corrosion process (corrosion occur mainly through surface macrodefects and the degradation of the film takes place on relatively large areas).

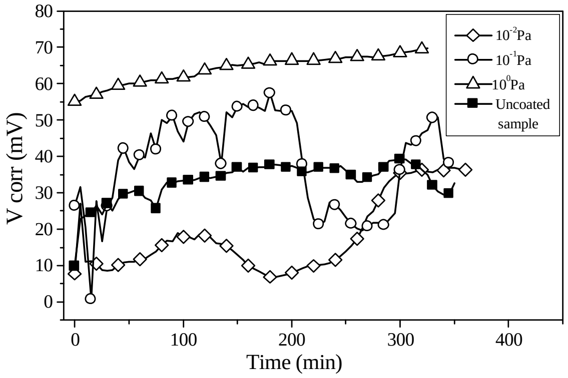

Fig. 3. Corrosion resistance for TiN coatings deposited by c.a.m. at different nitrogen pressures (V_s= 220 V).

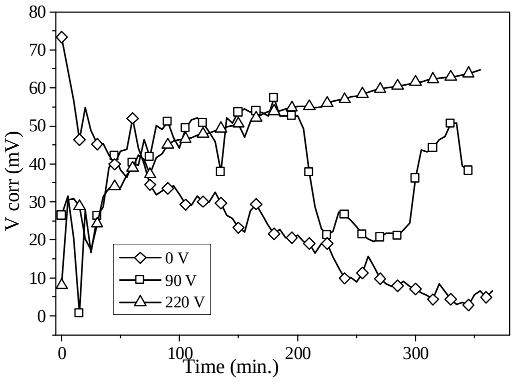

Fig. 4. Corrosion resistance for TiN coatings deposited by c.a.m at different substrate bias voltages ($p_{N2} = 3 \times 10^{-1}$ Pa).

These results can be understood if we take into account the chemical composition analysis (Table 3) and the surface topography examination (Fig. 5). It can be seen that the film stoichiometry insignificantly changes with the variation of N_2 pressure in the range 10^{-2} - 1 Pa. On the other hand, an increase in the nitrogen pressure leads to an improvement of the surface quality (pinholes, flaws, crater and droplet like defects are reduced while the N_2 pressure increased) and this effect can cause the observed corrosion behavior.

As it comes out from the Fig. 4, the corrosion resistance improved with the increase of the substrate bias. For the films deposited at low voltages (0-90 V) both pitting and crevice corrosion can be observed. A much better corrosion protection was found for the coating deposited at 220 V. Since previous experiments showed that both the chemical composition and the surface topography depends slightly on the substrate bias, the increase of the corrosion resistance with the bias is probably due to the fact that, as it is known (e.g. [13],[14]), an enhancement of the ion bombardment on the substrate results is a denser coating morphology. The beneficial effect of the ion bombardment on the corrosion protective properties of TiN and ZrN coatings has been also reported recently [15].

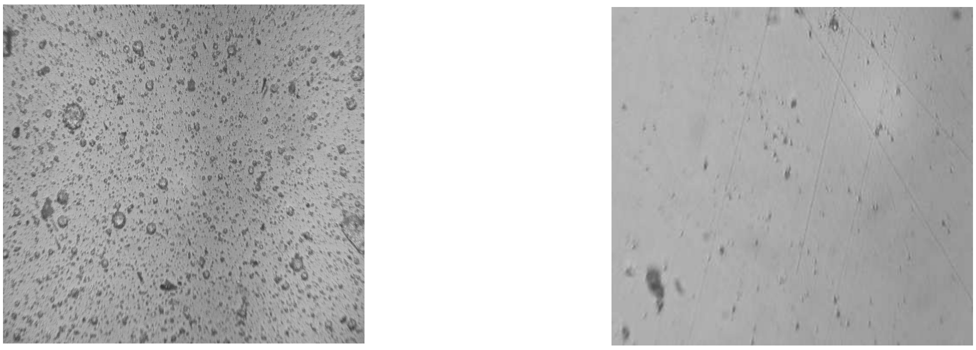

(a) $p_{N2} = 10^{-2}$ Pa (b) $p_{N2} = 1$ Pa

Fig. 5. Surface topography of TiN coatings deposited by c.a.m. at different nitrogen pressures (x 400).

3.4. Magnetron deposited films

The influence of the N_2 pressure on the corrosion behavior of the r.m.s.m. coatings is shown in Fig. 6. For the films deposited at N_2 pressure of 3 and 5×10^{-1} Pa, a relatively good corrosion protection was observed. The coatings exhibited similar evolutions of the potential (positive values) and only slight variations of the potential were recorded. A different behavior is to be found for the film prepared at 10^{-1} Pa: the potential has negative values, suggesting a low corrosion protection, and its variations in time indicate an increase of the anodic region area, probably due both to an increase of the coating porosity and to the coating flaking. Though the influence of the N_2 pressure on the corrosion behavior is similar for both deposition methods (an improvement of the corrosion resistance with the increase of the N_2 pressure) the reasons for this effect are different for the two methods. In contrast with the c.a.m. coatings, the variation of the N_2 pressure had no significant influence on the surface topography of the r.m.s.m. films, as shown in Fig. 8. The surfaces are smooth and only few defects can be observed. That is why for the r.m.s.m. coatings the influence of the N_2 pressure on the TiN stoichiometry must be taken into account. As it results from Table 3, the variation of the N_2 pressure in the range $10^{-1} - 5 \times 10^{-1}$ Pa led to a significant change of the N/Ti ratio in the film composition. One may conclude that a substoichiometric TiN film offers a worse corrosion protection in comparison to that of a stoichiometric or an overstoichiometric TiN film.

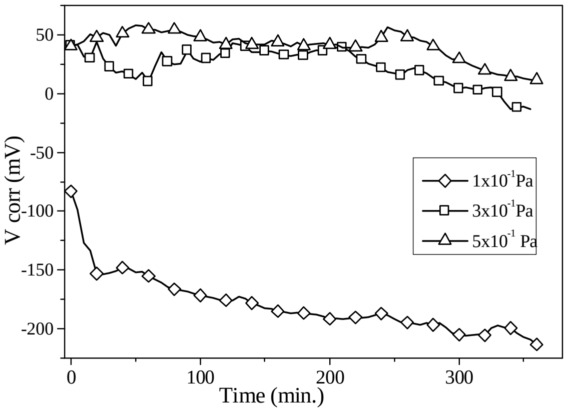

Fig. 6. Corrosion resistance for TiN Coatings deposited by r.m.s.m. at different nitrogen pressures (V_s=50V).

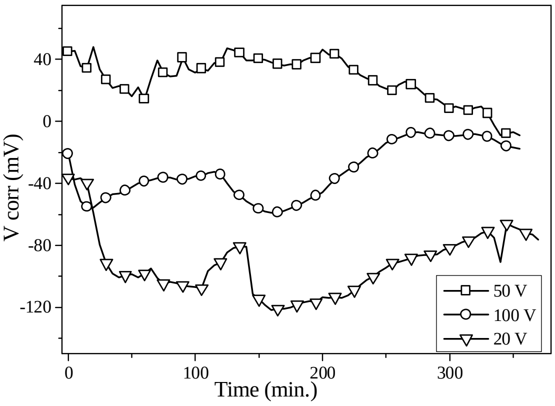

Fig. 7. Corrosion resistance for TiN coatings deposited by r.m.s.m. at different substrate bias voltages ($p_{N2} = 3 \times 10^{-1}$ Pa).

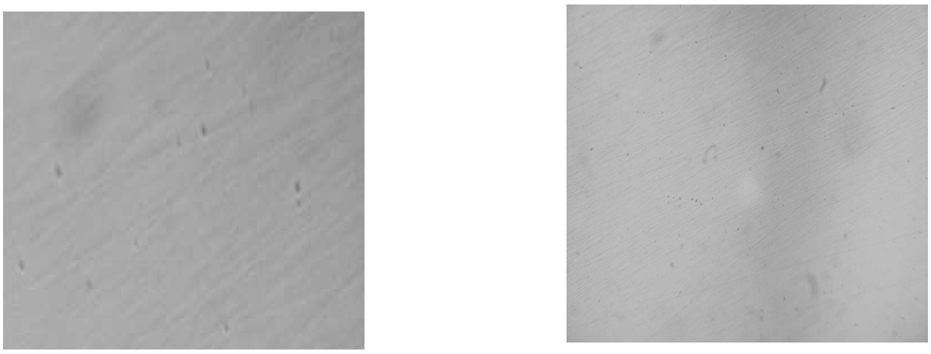

a) $p_{N2} = 10^{-1}$ Pa b) $p_{N2} = 5 \times 10^{-1}$ Pa

Fig. 8. Surface topography of TiN coatings deposited by r.m.s.m. at different nitrogen pressures (x400).

Substrate bias effect on the film corrosion resistance is illustrated in Fig. 7. The films deposited at bias voltages of 20 and 100 V exhibited a bad corrosion behavior: low negative potential values and fluctuations suggesting crevice corrosion processes. The best corrosion protection was obtained for the film prepared at an intermediate bias values, of 50 V. A possible explanation for this result can be found if we take into account the effects of the ion bombardment both on the film stoichiometry and on its microstructure. On one hand, for this deposition method an increase of the substrate bias acts in a similar manner as a decrease of the nitrogen pressure (the N/Ti ratio is diminished) [16], affecting the corrosion behavior, as it was pointed out above. One the other hand, a more intense ion bombardment leads to a more compact film structure. As a result of these combining effects, a narrow range of optimum values for the substrate bias is expected.

It is interesting to correlate the corrosion resistance of the TiN coatings with other film characteristics such as texture, microhardness or adhesion.

The existing studies showed that some properties of the TiN films (microhardness, adhesion, tribological performance) depend on their growth orientation [17], [18]. For example, the coatings with the (111) preferred orientation exhibited the best wear resistance [19]. Since all coatings studied in this work exhibited a pronounced (111) preferred orientation, it could not be evidenced the influence of the texture on the corrosion resistance of the films. Anyhow, as it was pointed out above, an (111) orientation is related to a high residual stress existing in the film and this commonly affects the coating adhesion [20]. As a result, one can suppose that these films exhibited a higher deterioration when exposed to corrosion environment in comparison with that of the films with (200) preferred orientation – for which the surface energy is dominant – or of the films exhibiting no preferred orientation. .

In contrast with the results of the corrosion test, the highest microhardness values were measured for the films deposited at relatively low pressures (10^{-2} Pa for c.a.m. and 10^{-1}Pa for r.m.s.m.)[7]. Therefore, since a high microhardness is commonly related to a high wear resistance, in the case of a certain application where the coated parts are subjected both to corrosion and wear, a compromise between corrosion and wear resistance must be chosen.

The experiments showed that the coatings with a poor adhesion (critical loads lower than 20-25N) exhibited also a low corrosion resistance (both pitting and crevice corrosion phenomena were evidenced).

4. Summary and conclusions

TiN coatings were deposited on 316L substrate by two different techniques (cathodic arc method (c.a.m.) and reactive magnetron sputtering method (r.m.s.m.)) in order to enhance the corrosion resistance in artificial physiological solution of austenitic stainless steels.

The corrosion resistance of the coatings deposited under various conditions was studied by means of an electrochemical test, consisting of measuring the time dependent variation of the free corrosion potential (OCP measurements). As reference, the corrosion behavior of an uncoated sample was presented. The coatings were also characterized with respect to elemental composition, phase composition, texture, surface topography, microhardness and adhesion.

The corrosion experiments showed that the corrosion behavior of the coatings prepared by both methods strongly depends on the main deposition parameters: N_2 pressure and substrate bias voltage. The increase of the nitrogen pressure (in the range 10^{-2} – 1 Pa and 10^{-1} – 5×10^{-1} Pa for c.a.m. and r.m.s.m., respectively) resulted in an improvement of the corrosion behavior of the film deposited by both methods. The influence of the substrate bias voltage on the film properties was different for these deposition techniques. In the case of c.a.m., the corrosion resistance has been improved by increasing the substrate bias in the range 20 – 200 V. For r.m.s.m., an optimum substrate bias, around 50 V, was found. These results were related to the influence of the deposition parameters on the chemical composition, surface topography and morphology of the coatings.

Of all coatings, only the samples prepared under very particular conditions (for c.a.m.: p_{N2} = 1 Pa, V_s = 220 V; for r.m.s.m.; p_{N2} = 5×10^{-1} Pa, V_s = 50 V) proved their capability to improve the corrosion-protective properties of the 316L substrate. Under the best deposition conditions, a superior corrosion resistance was observed for the coatings prepared by the cathodic arc system.

References

[1] D. Hill, Design Engineering of Biomaterials for Medical Devices, Ed.Wiley, New York (1998).
[2] D. Muster , Biocompatibilite et evolution de l`utilization des biomateriaux metaliques, in Actualites en Biomateriaux, vol. V, Ed. Romillat, Paris (2000).
[3] J. Helsen, H. Breme, Metals as Biomaterials, Ed. Wiley, New York (1998).
[4] Handbook of Deposition Technologies for Films and Coatings, Eds. R. F. Bunshah, 2nd ed., 1995.
[5] J. E. Sundgren, B. O. Johansson, S. E. Karlsson, Thin Solid Films **105**, 353 (1983).
[6] S. Chatterjee, T. S. Sudarshan, S. Chandrashekhar, J. Mat. Sci. **27**, 1989 (1992).
[7] M. Balaceanu, V. Braic, D. Macovei, M. Genet, A. Manea, D. Pantelica, M. Braic, F. Negoita, J. Optoelectron. Adv. Mater. **4**(1), 107 (2002).
[8] V. T. Braic, M. T. Braic, M. Popescu, C. D. Melinte, in Protective Coatings and Thin Filims, Eds.Y. Pauleau, P. B. Barna, Kluwer Academic Publishers, Dordecht/Boston/London 367 (1997).
[9] Jacques Brugerard, Étude du comportement électrochimique des métaux et alliages dentaires, Ed. Julien Prélat, Paris (1970).
[10] Handbook of Vacuum Arc Science and Technology, Ed. R. L. Boxman, D. M. Sanders, P. J. Martin, Noyes Publications, Park Ridge, N. J., U.S.A (1995).
[11] U. C. Oh, Jung Ho Je, J. Appl. Phys. **74** (3), 1692 (1993).
[12] J. Vyskočil, J. Musil, J.Vac.Technol. **A10** (4), 1740 (1992)
[13] V. Poulek, J. Musil, R. Cerny, R. Jr. Kusel, Thin Solid Films **170**, L55 (1989).
[14] K. S. Fancey, C. A. Porter, A. Matthews, J. Vac. Sci. Technol. **A13**, 428 (1995).
[15] E. Kelesoglu, C. Mitterer, M. Ürgen, Surf. Coat. Technol. **160**, 82 (2002).
[16] S. Logothetidis, I. Alexandrou, A. Papadopoulos, J. Appl. Phys. **77**(3), 1043 (1995).
[17] J. Musil, S. Kadlec, J. Vyskočil, V. Valvoda, Thin Solid Films **167**, 107 (1988).
[18] Nguyen Huy Hoang, D. R. Mc Kenzie, W. D. Mc Fall, Y. Yin, J. Appl. Phys. **80** (11), 6279 (1996).
[19] S. Veprek, Thin Solid Films **130**, 135 (1985).
[20] D. S. Rickerby, J. Vac. Sci. Technol. **A 4**(6), 2809 (1986).